Published in final edited form as:
Acta Crystallogr D Biol Crystallogr. 2004 August ; 60(Pt 8): 1456–1460.

Crystallization and preliminary analysis of active nitroalkane oxidase in three crystal forms

Akanksha Nagpal[a], **Michael P. Valley**[b], **Paul F. Fitzpatrick**[b], and **Allen M. Orville**[a]
a*School of Chemistry and Biochemistry, Georgia Institute of Technology, Atlanta, GA 30332-0400, USA*

b*Department of Biochemistry and Biophysics and Department of Chemistry, Texas A&M University, College Station, Texas 77843-2128, USA*

Abstract

Nitroalkane oxidase (NAO), a flavoprotein cloned and purified from *Fusarium oxysporum*, catalyzes the oxidation of neutral nitroalkanes to the corresponding aldehydes or ketones, with the production of H_2O_2 and nitrite. In this paper, the crystallization and preliminary X-ray data analysis of three crystal forms of active nitroalkane oxidase are described. The first crystal form belongs to a trigonal space group (either $P3_121$ or $P3_221$, with unit-cell parameters $a = b = 103.8$, $c = 487.0$ Å) and diffracts to at least 1.6 Å resolution. Several data sets were collected using 2θ and κ geometry in order to obtain a complete data set to 2.07 Å resolution. Solvent-content and Matthews coefficient analysis suggests that crystal form 1 contains two homotetramers per asymmetric unit. Crystal form 2 ($P2_12_12_1$; $a = 147.3$, $b = 153.5$, $c = 169.5$ Å) and crystal form 3 ($P3_1$ or $P3_2$; $a = b = 108.9$, $c = 342.5$ Å) are obtained from slightly different conditions and also contain two homotetramers per asymmetric unit, but have different solvent contents. A three-wavelength MAD data set was collected from selenomethionine-enriched NAO (SeMet-NAO) in crystal form 3 and will be used for phasing.

1. Introduction

Organic nitrochemicals are often difficult to metabolize, mutagenic or toxic and consequently occur only rarely from natural sources. However, when they are biosynthesized they are very often used as a chemical defense against pathogens (Clark et al., 1974; Hanawa et al., 2000). For example, nitropropionic acid, which is produced by some plants, inhibits succinate dehydrogenase and fumarase with very high affinity. Thus, its biocidal activity results in part by inhibition of the citric acid cycle of potential pathogens (Porter & Bright, 1980; Hassel & Sonnewald, 1995). Alternatively, the toxicity of many nitrochemicals originates from their metabolic transformation. The reduction of organic nitrochemicals by one, two or four electrons produces nitroradical anion, nitroso and hydroxylamino intermediates, respectively (Nathan & Shiloh, 2000). These types of reactive nitrogen intermediates are strong mutagens similar to nitrous acid and hydroxylamine, which readily modify DNA bases.

Correspondence e-mail: allen.orville@chemistry.gatech.edu.

This research was supported by funds from the Georgia Tech Research Corporation, the Georgia Institute of Technology Office of the Vice Provost for Research and an American Chemical Society Petroleum Research Fund type G grant (40310-G4) to AMO and by NIH grant GM58698 to PFF. Portions of this research were carried out at the Southeast Regional Collaborative Access Team (SER-CAT) beamline 22-ID at the Advanced Photon Source (APS), Argonne National Laboratory (SER-CAT supporting institutions may be found at http://www.ser-cat.org/members.html) and at the BioCARS sector 14 of APS (supported by the National Institutes of Health, National Center for Research Resources, under Grant RR07707). The use of APS is supported by the US Department of Energy, Basic Energy Sciences, Office of Science under Contract No. W-31-109-Eng-38. Preliminary diffraction data were also collected at beamline X26C of the National Synchrotron Light Source, Brookhaven National Laboratory, which is supported by the US Department of Energy, Division of Materials Sciences and Division of Chemical Sciences under Contract No. DE-AC02-98CH10886.

Despite their toxic characteristics, recent studies have established that many nitrochemicals are catabolized by prokaryotic and eukaryotic organisms as sources of nitrogen and/or carbon (Somerville et al., 1995; Spain, 1995; French et al., 1998; Hawari et al., 2000; Spain et al., 2000; Ebert et al., 2001; Rosser et al., 2001; Johnson et al., 2002; Seth-Smith et al., 2002; Trott et al., 2003). Indeed, several prokaryotic FMN-dependent enzymes have received recent attention because they reductively eliminate nitrite from xenobiotic explosive compounds, which can serve as a sole source of nitrogen (Spain, 1995; Binks et al., 1996; Blehert et al., 1997, 1999; French et al., 1998; Nivinskas et al., 2000; Riefler & Smets, 2000; Williams & Bruce, 2000; Barna et al., 2001; Ebert et al., 2001; Meah et al., 2001; Haynes et al., 2002; Johnson et al., 2002; Khan et al., 2002; Koder et al., 2002; Williams & Bruce, 2002; Orville, Manning, Blehert, Fox et al., 2004; Orville, Manning, Blehert, Studts et al., 2004). Thus, it appears that the reductive enzymes enable some microorganisms to exploit nitrochemicals introduced into the environment by recent human activities. In contrast, several FAD-dependent eukaryotic enzymes are known to catalyze oxidative nitrite eliminations from naturally occurring nitroaliphatic compounds (Kido, Soda et al., 1976; Kido, Yamamoto et al., 1976; Kido et al., 1978; Kido & Soda, 1978; Dhawale & Hornemann, 1979; Gadda & Fitzpatrick, 1999; Gadda, Choe et al., 2000). These enzymes appear to have evolved in parallel with organisms that produce nitrochemicals as a means to circumvent the chemical defenses of competing organisms within a particular niche.

Nitroalkane oxidase from *Fusarium oxysporum* (NAO) catalyzes reactions of the type

$$R - \mathrm{CH_2} - \mathrm{NO_2^-} + \mathrm{O_2} + \mathrm{H_2O} \rightarrow R - \mathrm{CHO} + \mathrm{NO_2^-} + \mathrm{H_2O_2} + \mathrm{H^+}.$$

The enzyme is induced when the fungus is grown on nitroethane as the sole nitrogen source (Kido et al., 1978). Although no crystal structures are currently available for NAO, structures are available for several NAO homologs, including the fatty acyl-CoA dehydrogenase (ACD) superfamily members rat short-chain ACD (Battaile et al., 2002), *Megasphaera elsdenii* butyryl-CoA dehydrogenase (Djordjevic et al., 1995), human medium-chain ACD (Lee et al., 1996), human isovaleryl-CoA dehydrogenase (Tiffany et al., 1997), pig liver mitochondria medium-chain ACD (Kim et al., 1993) and the most distant relative, rat liver peroxisomal acyl-CoA oxidase-II (ACO; Nakajima et al., 2002). To our knowledge, none of the ACD or ACO enzymes will transform nitroalkanes, nor will NAO transform acyl-CoA substrates (Daubner et al., 2002). Therefore, despite similar mechanistic features and primary sequence homology, there must be structural differences that prevent cross-reactivity between substrates of the different family members. Crystallographic analysis will thus provide mechanistic as well as potentially evolutionary insights into this family of proteins. To this end, we report the crystallization of active NAO in three crystal morphologies, including a selenomethionine-enriched form of NAO (SeMet-NAO). The X-ray diffraction data are of sufficient quality and resolution to support a crystal structure determination, which is in progress.

2. Material and methods

2.1. Protein expression and purification

Recombinant nitroalkane oxidase was expressed and purified from *Escherichia coli* strain BL21 (DE3) transformed with pETNAO4 as previously described (Daubner et al., 2002; Valley & Fitzpatrick, 2003b). The purified enzyme was stored in 20 m*M* HEPES pH 8.0, 1 m*M* EDTA, 5% glycerol and aliquots were flash-frozen with liquid N_2. SeMet-enriched NAO was obtained by expression in the methionine auxotroph *E. coli* B834(DE3) (Novagen) based on the procedure of Studts & Fox (1999). A single colony of *E. coli* B834(DE3) transformed with pETNAO4 was used to inoculate 5 ml of LB containing 100 μg ml^{-1} carbenicillin at 310 K. After 8 h, 1 ml of the starter culture was used to inoculate 50 ml of a minimal medium composed

of the following: 7.0 g l^{-1} Na_2HPO_4, 3.0 g l^{-1} KH_2PO_4, 1.0 g l^{-1} NH_4Cl, 0.1 g l^{-1} all amino acids, 0.1 g l^{-1} adenine, 0.002 g l^{-1} thiamine and riboflavin, 0.1 g l^{-1} carbenicillin, 2 m*M* $MgSO_4$, 0.1 m_M $CaCl_2$ and 22 m_M D-glucose. After 12 h at 310 K, 4 ml of the step-up culture was used to inoculate 1 l (6×) of the same minimal media, except that methionine was replaced with selenomethionine at 0.1 g l^{-1}. When the absorbance at 600 nm reached 0.6, the temperature of the cultures was lowered from 310 to 298 K and IPTG was added to a final concentration of 0.25 m*M*. Cells were harvested after 8.5 h expression and SeMet-enriched NAO was purified by the normal protocol. The gene sequence for NAO predicts a 439-amino-acid protein of 48 162 Da. The amino-terminal methionine is cleaved by the expression host, resulting in 13 methionines per chain. Biophysical solution studies are consistent with a homotetramer–homodimer equilibrium with a K_a for tetramerization of 8×10^6 M^{-1} (Gadda & Fitzpatrick, 1998).

2.2. Crystallization and X-ray diffraction data collection

Needle-shaped microcrystals were initially obtained from Cryoscreen HR-1 (Hampton Research, Aliso Viejo, CA, USA) with the hanging-drop vapor-diffusion method. These conditions were optimized and diffraction-quality crystals (form 1) were grown by mixing 2 µl 10 mg ml^{-1} protein solution (10 m*M* sodium cacodylate pH 7.5) with 2 µl of reservoir solution containing 25%(*w*/*v*) PEG 4000 and 35%(*v*/*v*) glycerol, 200 m*M* sodium cacodylate trihydrate pH 7.5, 1 m*M* spermine hydrochloride (Spm-Cl) at 277 K. The crystals typically grew within 10 d. NAO in crystal form 2 was grown from conditions containing 25%(*w*/*v*) PEG 4000 and 30%(*v*/*v*) glycerol, 200 m*M* sodium cacodylate trihydrate pH 7.5, 1 m*M* Spm-Cl and 8%(*w*/*v*) 1,6-hexanediol at 277 K. Single square-shaped crystals (0.15 × 0.12 mm) were obtained by mixing 2 µl of 8 mg ml^{-1} protein solution with 2 µl reservoir solution after 25–30 d equilibration at 277 K. Crystal form 3 was of SeMet-NAO enzyme and was grown from conditions similar to crystal form 1, except the protein was incubated at 277 K for 5 h with 10 m*M* dithiothreitol prior to setting up the drop. The SeMet-NAO crystals typically grew within two weeks. For each crystal form, single crystals were mounted directly in nylon loops as no additional cryoprotectant was necessary and they were flash-frozen by quick submersion into liquid N_2. All X-ray diffraction data were collected from crystals held at approximately 100 K.

Several data sets from two crystals were merged to yield a complete high-resolution data set for crystal form 1. The data-collection strategy consisted of three or four data-collection sweeps using 0.90 Å X-rays, a 30 s exposure per frame and an ADSC Quantum 4 detector at BioCARS beamline 14-BMC of the Advanced Photon Source (APS) at Argonne National Laboratory. The highresolution data were collected with a 0.3° rotation per frame, κ geometry, a 150 mm vertical detector offset and a 400 mm crystal-to-detector distance. The low-resolution data were collected with similar settings but without a vertical detector offset.

X-ray diffraction data from crystal form 2 were collected at the SER-CAT sector of APS on beamline 22-ID using a MAR CCD 165 detector. Each image was collected using 1.0 Å X-rays with a crystal-to-detector distance of 250 mm. A total of 180° of φ rotation was collected with a 2 s exposure time per frame and a 0.5° oscillation range.

A three-wavelength MAD data set was collected from SeMet-NAO at SER-CAT using a MAR 225 detector. A high-sensitivity fluorimeter (Röntec USA Inc., Carlisle, MA, USA) was used to separate the arsenate peak from the selenium signal. Forward- and inverse-beam data sets (110° of φ rotation each) were collected at the peak (0.9792 Å), inflection (0.9794 Å) and remote (0.9686 Å) wavelengths. Each frame was collected with an exposure time of 4 s and a 1.0° oscillation range. The crystal-to-detector distance was 270 mm.

Data sets for crystal forms 1 and 3 were processed with *HKL2000* (Otwinowski & Minor, 1997). The data sets for crystal form 2 were processed with *MOSFLM* (Powell, 1999) and *SCALA* from the *CCP4* suite of programs (Collaborative Computational Project, Number 4, 1994). The three-wavelength MAD data set of SeMet-NAO was further scaled and analyzed with *FHSCALE* and *SCALEIT* from the *CCP4* suite of programs.

3. Results and discussion

NAO has been crystallized in three crystal forms as described above and illustrated in Fig. 1. In each case the crystals were bright yellow, suggesting the presence of oxidized FAD in the active site. Each crystal form diffracts X-rays to at least 3.2 Å resolution and the data-collection statistics are presented in Table 1. Crystal form 1 is remarkable because the unit cell has a 487 Å *c* unit-cell parameter and typically displays a relatively low mosaic spread. As of 6 April 2004, the PDB contained only 216 X-ray structures (out of 21 305) with any unit-cell parameter greater than 450 Å (Berman et al., 2002,2003;Bourne et al., 2004). Moreover, only 18 of these structures were reported to a resolution equal to or higher than 2.5 Å; the vast majority were reported to a resolution of lower than 3.0 Å. In contrast, we have observed that crystal form 1 of NAO often diffracts to at least 1.6 Å resolution at several synchrotron X-ray sources (data not shown). However, the unit-cell parameters pushed the limits of the data-collection facilities available at several synchrotron X-ray facilities. Thus, a complete data set to the observed high-resolution limit has not yet been achieved. Nevertheless, a complete data set to 2.07 Å resolution has been obtained by merging data from several data-collection passes from two crystals as described above. Solvent-content and Matthews coefficient analysis (Matthews, 1968;Kantardjieff & Rupp, 2003) in space group $P3_121$ or $P3_221$ suggest that there are most likely to be six NAO chains in the asymmetric unit (four chains, V_M = 3.95 Å^3 Da^{-1}, 68.90% solvent; six chains, V_M = 2.64 Å^3 Da^{-1}, 53.4% solvent; eight chains, V_M = 1.98 Å^3 Da^{-1}, 37.8% solvent). Local symmetry relating the chains in the asymmetric unit is anticipated and will be employed during model building and refinement of each 438-amino-acid residue chain.

Slight alterations of the crystallization conditions yielded crystals with visibly different morphologies (Fig. 1). Analysis of X-ray diffraction data revealed that the unit-cell parameters were also different to those of crystal form 1. As described above and shown in Table 1, addition of 1,6-hexanediol induced crystal form 2. The orthorhombic space group demonstrated systematic absences along all three principal axes, which was consistent with space group $P2_12_12_1$. The solvent content and Matthews coefficient analysis suggested that there were most likely to be eight NAO chains in the asymmetric unit (six chains, V_M = 3.33 Å^3 Da^{-1}, 60.1% solvent; eight chains, V_M = 2.5 Å^3 Da^{-1}, 50.7% solvent).

Crystal form 3 grew with SeMet-enriched NAO and conditions that included DTT but otherwise typically yielded crystal form 1. The resulting space group was trigonal and the merging statistics and systematic absences suggested either $P3_1$ or $P3_2$. Thus, crystal form 3 does not have crystallographic twofold symmetry along the *a* unit-cell edge and the *c* edge was significantly shorter than the trigonal cell in crystal from 1 (Table 1). Based on solvent-content and Matthews coefficient analysis, there were most likely to be ten NAO chains in the asymmetric unit (eight chains, V_M = 3.04 Å^3 Da^{-1}, 59.6% solvent; ten chains, V_M = 2.44 Å^3 Da^{-1}, 49.5% solvent; 12 chains, V_M = 2.03 Å^3 Da^{-1}, 39.4% solvent). Despite the presence of arsenate in the sodium cacodylate buffer system, a three-wavelength MAD data set was collected at the peak, inflection and remote energies. Preliminary analysis of the MAD data with *SCALEIT* revealed that the dispersive differences were smallest between the reflections collected at the peak and the inflection energies (normal probability for acentric reflections = 1.357) and largest between the inflection point and the high-energy remote energies (normal probability for acentric reflections = 2.099). The data analysis also suggested that the anomalous differences were highest for the peak-data set (normal probability for acentric

reflections = 1.934). Phase determination of the SeMet-NAO data will be complex since there are up to 104 SeMet sites anticipated. They will be located and refined with a parallel version of *Shake-and-Bake* (Hauptman, 1997;Howell et al., 2000;Xu et al., 2002), *SOLVE* (Terwilliger & Berendzen, 1999) or *SHARP* (de La Fortelle & Bricogne, 1997) and the results will be reported elsewhere.

NAO has recently been identified as a new member of the fatty acyl-CoA dehydrogenase superfamily, but only shares approximately 23–27% pairwise amino-acid sequence identity to other family members (Daubner et al., 2002; Valley & Fitzpatrick, 2003a,b). Different ACDs discriminate between fatty-acid substrates of four to more than 18 C atoms in length (Thorpe & Kim, 1995; Stankovich et al., 1999; Battaile et al., 2002). The best homologs of NAO are the homotetrameric medium- and short-chain ACDs, which prefer substrates with less than eight C atoms. Accordingly, NAO exhibits a relatively broad substrate tolerance, with primary nitroalkanes of four, five or six C atoms in length among the most catalytically proficient substrates (relative *V/K*; Gadda & Fitzpatrick, 1998, 1999, 2000a,b; Gadda, Banerjee, Dangott et al., 2000; Gadda et al., 2000; Gadda, Choe et al., 2000). NAO also demonstrates a strong preference for neutral substrates, which differentiates it from other flavoenzymes that transform nitroalkane anions, such as 2-nitropropane dioxygenase and D-amino-acid oxidase (Porter et al., 1972; Kido, Soda et al., 1976; Kido, Yamamoto et al., 1976; Porter & Bright, 1977; Kido et al., 1978; Kido & Soda, 1978; Gorlatova et al., 1998). Although the O_2 reactivity of NAO is not a characteristic of its ACD homologs, it is analogous to peroxisomal acyl-CoA oxidase (ACO). ACO is a homodimeric enzyme with an approximately 440 amino-acid N-terminal FAD domain that is structurally homologous to the ACDs (Nakajima et al., 2002), but shares only approximately 7% primary sequence similarity to NAO. Thus, whereas the ACDs transfer reducing equivalents to the electron-transport chain, the ACO and NAO in contrast react with O_2 to complete the reaction cycle (Fitzpatrick, 2001). In the catalytic cycles of all three enzymes, a base abstracts an acidic proton to initiate catalysis, but the subsequent steps differ. In ACO and ACD, proton abstraction from the α-carbon is accompanied by hydride transfer from the β-carbon to the flavin in a concerted reaction. In NAO, the anion is a true intermediate which adds to the N5 position of the flavin. Thus, the crystal structure of NAO will provide important insights into how similar flavoenzyme active sites yield different reaction coordinates.

References

Barna TM, Khan H, Bruce NC, Barsukov I, Scrutton NS, Moody PC. J. Mol. Biol 2001;310:433–447. [PubMed: 11428899]

Battaile KP, Molin-Case J, Paschke R, Wang M, Bennett D, Vockley J, Kim JJ. J. Biol. Chem 2002;277:12200–12207. [PubMed: 11812788]

Berman HM, Battistuz T, Bhat TN, Bluhm WF, Bourne PE, Burkhardt K, Feng Z, Gilliland GL, Iype L, Jain S, Fagan P, Marvin J, Padilla D, Ravichandran V, Schneider B, Thanki N, Weissig H, Westbrook JD, Zardecki C. Acta Cryst 2002;D58:899–907.

Berman H, Henrick K, Nakamura H. Nature Struct. Biol 2003;10:980. [PubMed: 14634627]

Binks PR, French CE, Nicklin S, Bruce NC. Appl. Environ. Microbiol 1996;62:1214–1219. [PubMed: 8919782]

Blehert DS, Fox BG, Chambliss GH. J. Bacteriol 1999;181:6254–6263. [PubMed: 10515912]

Blehert DS, Knoke KL, Fox BG, Chambliss GH. J. Bacteriol 1997;179:6912–6920. [PubMed: 9371434]

Bourne PE, Addess KJ, Bluhm WF, Chen L, Deshpande N, Feng Z, Fleri W, Green R, Merino-Ott JC, Townsend-Merino W, Weissig H, Westbrook J, Berman HM. Nucleic Acids Res 2004;32:D223–D225. [PubMed: 14681399]

Clark NG, Croshaw B, Leggetter BE, Spooner DF. J. Med. Chem 1974;17:977–981. [PubMed: 4370420]

Collaborative Computational Project. Acta Cryst 1994;D50:760–763.Number 4

Daubner SC, Gadda G, Valley MP, Fitzpatrick PF. Proc. Natl Acad. Sci. USA 2002;99:2702–2707. [PubMed: 11867731]

Dhawale MR, Hornemann U. J. Bacteriol 1979;137:916–924. [PubMed: 33965]

Djordjevic S, Pace CP, Stankovich MT, Kim JJ. Biochemistry 1995;34:2163–2171. [PubMed: 7857927]

Ebert S, Fischer P, Knackmuss HJ. Biodegradation 2001;12:367–376. [PubMed: 11995829]

Fitzpatrick PF. Acc. Chem. Res 2001;34:299–307. [PubMed: 11308304]

French CE, Nicklin S, Bruce NC. Appl. Environ. Microbiol 1998;64:2864–2868. [PubMed: 9687442]

Gadda G, Banerjee A, Dangott LJ, Fitzpatrick PF. J. Biol. Chem 2000;275:31891–31895. [PubMed: 10913134]

Gadda G, Banerjee A, Fitzpatrick PF. Biochemistry 2000;39:1162–1168. [PubMed: 10653664]

Gadda G, Choe DY, Fitzpatrick PF. Arch. Biochem. Biophys 2000;382:138–144. [PubMed: 11051107]

Gadda G, Fitzpatrick PF. Biochemistry 1998;37:6154–6164. [PubMed: 9558355]

Gadda G, Fitzpatrick PF. Arch. Biochem. Biophys 1999;363:309–313. [PubMed: 10068453]

Gadda G, Fitzpatrick PF. Biochemistry 2000a;39:1400–1405. [PubMed: 10684620]

Gadda G, Fitzpatrick PF. Biochemistry 2000b;39:1406–1410. [PubMed: 10684621]

Gorlatova N, Tchorzewski M, Kurihara T, Soda K, Esaki N. Appl. Environ. Microbiol 1998;64:1029–1033. [PubMed: 9501443]

Hanawa F, Tahara S, Towers GH. Phytochemistry 2000;53:55–58. [PubMed: 10656408]

Hassel B, Sonnewald U. J. Neurochem 1995;65:1184–1191. [PubMed: 7643096]

Hauptman HA. Methods Enzymol 1997;277:3–13. [PubMed: 9379923]

Hawari J, Halasz A, Sheremata T, Beaudet S, Groom C, Paquet L, Rhofir C, Ampleman G, Thiboutot S. Appl. Environ. Microbiol 2000;66:2652–2657. [PubMed: 10831452]

Haynes CA, Koder RL, Miller AF, Rodgers DW. J. Biol. Chem 2002;277:11513–11520. [PubMed: 11805110]

Howell PL, Blessing RH, Smith GD, Weeks CM. Acta Cryst 2000;D56:604–617.

Johnson GR, Jain RK, Spain JC. J. Bacteriol 2002;184:4219–4232. [PubMed: 12107140]

Kantardjieff KA, Rupp B. Protein Sci 2003;12:1865–1871. [PubMed: 12930986]

Khan H, Harris RJ, Barna T, Craig DH, Bruce NC, Munro AW, Moody PC, Scrutton NS. J. Biol. Chem 2002;277:21906–21912. [PubMed: 11923299]

Kido T, Hashizume K, Soda K. J. Bacteriol 1978;133:53–58. [PubMed: 22538]

Kido T, Soda K. J. Biol. Chem 1978;253:226–232. [PubMed: 201619]

Kido T, Soda K, Suzuki T, Asada K. J. Biol. Chem 1976;251:6994–7000. [PubMed: 11214]

Kido T, Yamamoto T, Soda K. J. Bacteriol 1976;126:1261–1265. [PubMed: 947888]

Kim JJ, Wang M, Paschke R. Proc. Natl Acad. Sci. USA 1993;90:7523–7527. [PubMed: 8356049]

Koder RL, Haynes CA, Rodgers ME, Rodgers DW, Miller AF. Biochemistry 2002;41:14197–14205. [PubMed: 12450383]

La Fortelle, E. de; Bricogne, G. Methods Enzymol 1997;276:472–494.

Lee HJ, Wang M, Paschke R, Nandy A, Ghisla S, Kim JJ. Biochemistry 1996;35:12412–12420. [PubMed: 8823176]

Matthews BW. J. Mol. Biol 1968;33:491–497. [PubMed: 5700707]

Meah Y, Brown BJ, Chakraborty S, Massey V. Proc. Natl Acad. Sci. USA 2001;98:8560–8565. [PubMed: 11438708]

Nakajima Y, Miyahara I, Hirotsu K, Nishina Y, Shiga K, Setoyama C, Tamaoki H, Miura R. J. Biochem. (Tokyo) 2002;131:365–374. [PubMed: 11872165]

Nathan C, Shiloh MU. Proc. Natl Acad. Sci. USA 2000;97:8841–8848. [PubMed: 10922044]

Nivinskas H, Koder RL, Anusevicius Z, Sarlauskas J, Miller AF, Cenas N. Acta Biochim. Pol 2000;47:941–949. [PubMed: 11996117]

Orville AM, Manning L, Blehert DS, Fox BG, Chambliss GH. Acta Cryst 2004;D60:1289–1291.

Orville AM, Manning L, Blehert DS, Studts JM, Fox BG, Chambliss GH. Acta Cryst 2004;D60:957–961.

Otwinowski Z, Minor W. Methods Enzymol 1997;276:307–326.

Porter DJ, Bright HJ. J. Biol. Chem 1977;252:4361–4370. [PubMed: 16930]

Porter DJ, Bright HJ. J. Biol. Chem 1980;255:4772–4780. [PubMed: 7372610]

Porter DJ, Voet JG, Bright HJ. Z. Naturforsch. B 1972;27:1052–1053. [PubMed: 4405074]

Powell HR. Acta Cryst 1999;D55:1690–1695.

Riefler RG, Smets BF. Environ. Sci. Technol 2000;34:3900–3906.

Rosser SJ, Basran A, Travis ER, French CE, Bruce NC. Adv. Appl. Microbiol 2001;49:1–35. [PubMed: 11757347]

Seth-Smith HM, Rosser SJ, Basran A, Travis ER, Dabbs ER, Nicklin S, Bruce NC. Appl. Environ. Microbiol 2002;68:4764–4771. [PubMed: 12324318]

Somerville CC, Nishino SF, Spain JC. J. Bacteriol 1995;177:3837–3842. [PubMed: 7601851]

Spain JC. Annu. Rev. Microbiol 1995;49:523–555. [PubMed: 8561470]

Spain, JC.; Hughes, JB.; Knackmuss, H-J., editors. Metabolism of Nitroaromatics and Explosive Compounds. CRC Press; Boca Raton, FL, USA: 2000.

Stankovich MT, Sabaj KM, Tonge PJ. Arch. Biochem. Biophys 1999;370:16–21. [PubMed: 10496972]

Studts JM, Fox BG. Protein Expr. Purif 1999;16:109–119. [PubMed: 10336868]

Terwilliger TC, Berendzen J. Acta Cryst 1999;D55:849–861.

Thorpe C, Kim JJ. FASEB J 1995;9:718–725. [PubMed: 7601336]

Tiffany KA, Roberts DL, Wang M, Paschke R, Mohsen AW, Vockley J, Kim JJ. Biochemistry 1997;36:8455–8464. [PubMed: 9214289]

Trott S, Nishino SF, Hawari J, Spain JC. Appl. Environ. Microbiol 2003;69:1871–1874. [PubMed: 12620886]

Valley MP, Fitzpatrick PF. J. Am. Chem. Soc 2003a;125:8738–8739. [PubMed: 12862464]

Valley MP, Fitzpatrick PF. Biochemistry 2003b;42:5850–5856. [PubMed: 12741843]

Williams, RE.; Bruce, NC. Biodegradation of Nitroaromatic Compounds and Explosives. Spain, JC.; Hughes, JB.; Knackmuss, H-J., editors. CRC Press; Boca Raton, FL, USA: 2000. p. 161-184.

Williams RE, Bruce NC. Microbiology 2002;148:1607–1614. [PubMed: 12055282]

Xu H, Hauptman HA, Weeks CM. Acta Cryst 2002;D58:90–96.

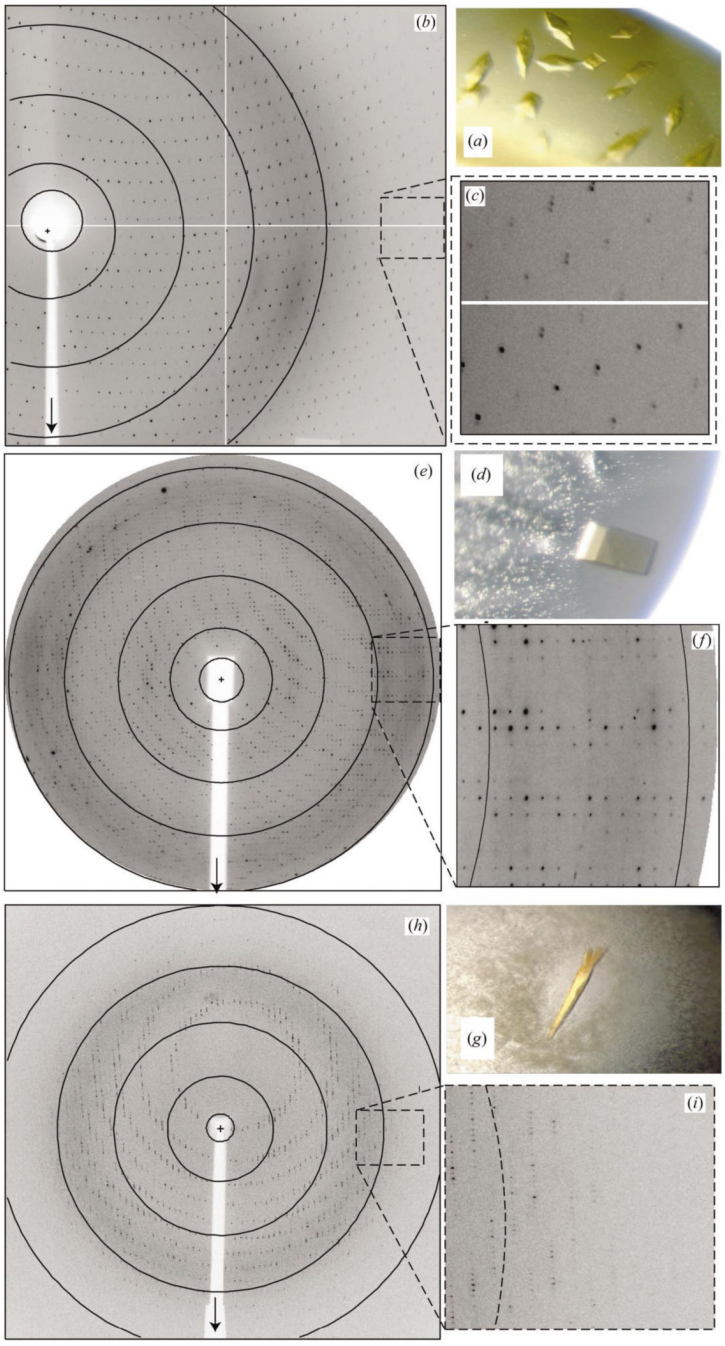

Figure 1.

Crystals photographed without polarization of nitroalkane oxidase (NAO) in (*a*) crystal form 1 (0.25 × 0.15 mm) and (*d*) crystal form 2 (0.15 × 0.12 mm) and (*g*) of SeMet-enriched NAO (0.3 × 0.1 mm) in crystal form 3. X-ray diffraction patterns at 100 K with rotation about the vertical axis (arrows) are shown in (*b*), (*e*) and (*h*). (*b*) was collected from (*a*) with an ADSC Quantum 4 detector at BioCARS beamline 14-BMC with 30 s exposure, 0.3° φ rotation and 400 mm crystal-to-detector distance; arcs indicate 3.5, 4.6, 6.9 and 13.8 Å, 2θ detector offset = 10.7°. (*e*) was collected from (*d*) with a MAR CCD 165 detector at SER-CAT beamline 22-ID, 2 s exposure, 0.5° φ rotation, 250 mm crystal-to-detector distance; circles indicate 3.2, 4.5,

6.8 and 13.6 Å. (*h*) was collected from (*g*) with a MAR CCD 225 detector at SER-CAT, 4 s exposures, 1.0° φ rotation, 270 mm crystal-to-detector distance; circles indicate 2.4, 3.3, 4.9 and 9.8 Å. Expanded and contrast-adjusted views of the high-resolution diffraction perpendicular to the rotation axis are shown in (*c*) from (*b*), 2.5 Å at the edge, (*f*) from (*e*), 3.2 Å at the edge and (*i*) from (*h*), 2.4 Å at the edge.

Table 1

Typical data-collection statistics for nitroalkane oxidase.Values for the highest resolution shell of data are given in parentheses.

Crystal form	**1**	**2**	**3 (SeMet)**	**3 (SeMet)**	**3 (SeMet)**
X-ray source	BIOCARS	SER-CAT	SER-CAT	SER-CAT	SER-CAT
Beamline	14-BMC	22-ID	22-ID	22-ID	22-ID
Wavelength (Å)	0.90	1.0032	0.9792 (peak)	0.9794 (inflection)	0.9686 (remote)
Detector	Quantum 4R	MAR CCD 165	MAR CCD 225	MAR CCD 225	MAR CCD 225
Resolution range (Å)	50–2.07 (2.15–2.07)	35–3.2 (3.4–3.2)	50–2.8 (2.9–2.8)	50–2.8 (2.9–2.8)	50–2.8 (2.9–2.8)
Mosaic spread (°)	~0.4	~0.6	~0.3	~0.3	~0.3
Space group	$P3_121$ or $P3_221$	$P2_12_12_1$	$P3_1$ or $P3_2$	$P3_1$ or $P3_2$	$P3_1$ or $P3_2$
Unit-cell parameters					
a (Å)	103.8	147.3	108.9	108.8	109.0
b (Å)	103.8	153.5	108.9	108.8	109.0
c (Å)	487.0	169.5	342.5	343.2	342.3
Total reflections	570374	239001	767349	787263	690400
Unique reflections	371128	55534	111892	111132	111156
Multiplicity	1.5 (1.0)	4.3 (2.7)	6.9 (5.2)	7.1 (6.4)	6.2 (4.5)
Completeness (%)	93.5 (80.0)	92.6 (92.6)	99.9 (99.6)	99.9 (99.8)	99.9 (99.8)
$R_{sym}(I)^{\dagger}$	0.139 (0.30)	0.073 (0.29)	0.126 (0.39)	0.126 (0.44)	0.147 (0.37)
$I/\sigma(I)^{\ddagger}$	12.6 (3.0)	7.8 (2)	11.4 (3.7)	11.8 (3.5)	11.5 (3.2)

$^{\dagger}R_{sym}(I)$ gives the average agreement between the independently measured intensities.

$^{\ddagger}I/\sigma(I)$ is the root-mean-square value of the intensity measurements divided by their estimated standard deviation.